Journal of Hazardous Materials 165 (2009) 664–669

Contents lists available at ScienceDirect

Journal of Hazardous Materials

journal homepage: www.elsevier.com/locate/jhazmat

Catalytic reduction of 4-nitrophenol by magnetically recoverable Au nanocatalyst

Yang-Chuang Chang, Dong-Hwang Chen*

Department of Chemical Engineering, National Cheng Kung University, Tainan 701, Taiwan

ARTICLE INFO

Article history:
Received 4 July 2008
Received in revised form
27 September 2008
Accepted 8 October 2008
Available online 18 October 2008

Keywords:
Nitrophenol
Catalytic reduction
Gold
Magnetic recoverable catalyst

ABSTRACT

A novel magnetically recoverable Au nanocatalyst was fabricated by the simple adsorption–reduction of Au(III) ions on chitosan-coated iron oxide magnetic nanocarrier. Au nanoparticles with a mean diameter of 3.14 nm were well loaded on the surface of magnetic nanocarrier because chitosan layer provided an effective driving force in the formation and stabilization of Au nanoparticles. The resultant magnetically recoverable Au nanocatalyst exhibited excellent catalytic activity to the reduction of 4-nitrophenol (4-NP) with sodium borohydride. The rate constants evaluated in terms of pseudo-first-order kinetic model increased with increasing the amount of Au nanocatalyst, decreasing the initial 4-NP concentration, and increasing the temperature. Also, the kinetic data suggested that this catalytic reaction was diffusion controlled owing to the presence of chitosan layer. In addition, catalyst reuse showed no trace of deactivation or poisoning during the catalytic and separation processes, revealing the stable nature and good catalytic ability of this nanocatalyst.

1. Introduction

Nitrophenols are among the most common organic pollutants in industrial and agricultural wastewaters. Many processes have been developed for their removal such as adsorption [1], microbial degradation [2], photocatalytic degradation [3], microwave-assisted catalytic oxidation [4], electro-Fenton method [5], electrocoagulation [6], electrochemical treatment [7] and so on. On the other hand, 4-aminophenol (4-AP) is an important intermediate for the manufacture of analgesic and antipyretic drugs. They can be synthesized by the catalytic hydrogenation of 4-nitrophenol (4-NP) in ethanol at relatively high temperature and high hydrogen pressure [8,9]. However, due to the reasons of energy saving, safe operation, and avoiding the use of organic solvents, it may be interesting and meaningful to develop the process for the conversion of 4-NP to 4-AP in aqueous solution under mild condition. Also, the process maybe could be used for the treatment of wastewater which contains mainly 4-NP without complicated composition.

In the past two decades, nanotechnology has been developed quickly in various fields. Nanoparticles have potential applications in chemistry, physics, electronics, biology, and medicine due to their unique characteristics different from bulk materials. One of the interesting studies of nanoparticles is of noble metal nanoparticles. Metal particles with size in nanometer regime have higher Fermi potential which leads to the lowering of reduction potential value, and hence metal nanoparticles can function as a catalyst for many electron-transfer reactions [10–12]. In the previous studies, the reduction of aromatic nitro compounds or dyes catalyzed by the noble metal nanoparticles stabilized with surfactant or dendrimer has been reported [13–19]. However, the recovery of noble metal nanoparticles from such stabilizers-containing systems is not easy and also makes the process of monitoring the reaction by a UV/VIS spectrophotometer extremely difficult due to the presence of suspended nanoparticles in reaction solution.

Magnetic carriers have been extensively used in the fields of metal ions and dyes recovery, drug delivery, enzyme immobilization, protein and cell separation, and so on [20–27], since magnetic separation technique possesses the advantages of rapidity, high efficiency, and cost-effectiveness. Recently, magnetic nanoparticles have emerged as robust, readily available, high-surface-area heterogeneous supports in catalytic transformations. They possess the added advantage of being magnetically recoverable, thereby eliminating the requirement for either solvent swelling before or catalyst filtration after the reaction [28].

The science of catalysis by gold is an area of considerable scientific exploration particularly with respect to developing new gold catalysts [29–33]. As has been known, the Au nanoparticles supported on the magnetic nanocarrier can serve as the electron relay between 4-nitrophenolate ion (oxidant) and BH_4^- (reductant), and electron transfer occurs via the Au nanoparticles [34,35]. Although a few studies on the catalytic properties of supported metal catalysts in colloidal solutions have been reported [36,37], relatively

---

* Corresponding author. Tel.: +886 6 2757575x62680; fax: +886 6 2344496.
E-mail address: chendh@mail.ncku.edu.tw (D.-H. Chen).

0304-3894/$ – see front matter © 2008 Elsevier B.V. All rights reserved.
doi:10.1016/j.jhazmat.2008.10.034

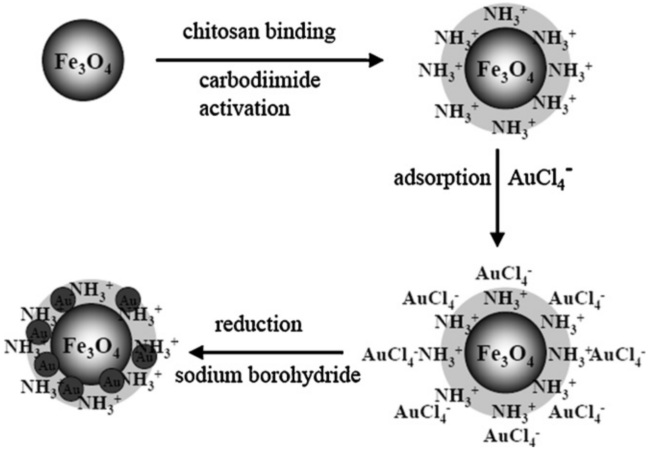

Fig. 1. An illustration for the fabrication of magnetically recoverable Au nanocatalyst by the adsorption–reduction of Au(III) ions on chitosan-coated iron oxide magnetic nanocarrier.

less efforts have been made on the fabrication and catalytic properties of metal nanoparticles supported on the magnetic nanocarrier. Recently we have developed a chitosan-coated magnetic nano-adsorber which has been shown to be quite useful for the recovery of metal ions (Cu(II), Co(II), and Au(III)) and dyes from the aqueous solutions and also suitable as a multifunctional magnetic nanocarrier for cancer therapy [20–24]. So, in the present study, we further developed a novel magnetically recoverable Au nanocatalyst by the simple adsorption–reduction of Au(III) ions on the chitosan-coated magnetic nano-adsorber as illustrated in Fig. 1. Its catalytic activity for the reduction of 4-NP to 4-AP with sodium borohydride was studied. Its reusability and the corresponding kinetic and thermodynamic properties were also investigated.

2. Materials and methods

2.1. Materials

Ferric chloride hexahydrate was the product of J.T. Baker (Phillipsburg). Ferrous chloride tetrahydrate, chitosan (low-viscous), sodium borohydride, and 4-nitrophenol were obtained from Fluka (Buchs). Ammonium hydroxide (29.6%) was supplied by TEDIA (Fairfield). Carbodiimide was purchased from Sigma Chemical Co. (St. Louis, MO). Hydrogen tetrachloroaurate was supplied by Alfa Aesar (Ward Hill). All chemicals were of guaranteed or analytical grade reagents commercially available and used without further purification. The water used throughout this work was the reagent-grade water produced by a Milli-Q SP ultra-pure-water purification system of Nihon Millipore Ltd., Tokyo.

2.2. Fabrication of magnetically recoverable Au nanocatalyst

Chitosan-coated magnetic nanocarrier was prepared according to our previous work [20]. Fe_3O_4 nanoparticles were prepared by co-precipitating method and chitosan was carboxymethylated. For the binding of carboxymethyl chitosan, 100 mg of Fe_3O_4 nanoparticles were first added to 2 mL of buffer A (0.003 M phosphate, pH 6, 0.1 M NaCl). Then, the reaction mixture was sonicated for 10 min after adding 0.5 mL of carbodiimide solution (0.025 g/mL in buffer A). Finally, 2.5 mL of carboxymethyl chitosan solution (50 mg/mL in buffer A) was added and the reaction mixture was sonicated for 60 min. The product was recovered from the reaction mixture by a permanent magnet, and then washed with water and ethanol. The resultant chitosan-coated magnetic nanocarrier has a mean diameter of 13.5 nm, 4.92 wt% chitosan, and an isoelectric point of 5.95. The characterization methods and other properties could be obtained in our previous works [16,17,19,20].

The magnetically recoverable Au nanocatalyst was fabricated as follows. First, 105.17 mg magnetic nanocarrier (i.e., 5.17 mg chitosan on 100 mg Fe_3O_4) obtained according to the above was added to 5 mL of hydrogen tetrachloroaurate solution. The maximum amount of Au(III) ions that could be adsorbed on the magnetic nanocarrier was studied in an aqueous solution of pH 2 at 25 °C by taking a fixed amount of magnetic nanocarrier and varying the concentration of Au(III) ions. The concentrations of Au(III) ions in solution before and after the adsorption process were determined by using a GBC Avanta atomic absorption spectrometer. After adsorption equilibrium, the magnetic nanocarrier was recovered by a permanent magnet with a surface magnetization of 6000 gauss, and then dispersed in 5 mL of deionized water. Secondly, in the aqueous media containing Au(III) ions-adsorbed magnetic nanocarrier, excessive $NaBH_4$ solution (50 mL, 0.01 M) was added and the reaction was carried out for about 10 min. The resultant magnetically recoverable Au nanocatalyst was recovered by using an external magnetic field, and then dispersed in 5 mL of deionized water. Its size and morphology were observed by transmission electron microscopy (TEM) performed on a JEOL Model JEM-1200EX at 80 kV.

2.3. Catalytic reduction of 4-NP

To investigate the catalytic reduction of 4-NP, 0.5 mL of solution-containing magnetically recoverable Au nanocatalyst was mixed with 4-NP and the volume of the mixture was adjusted to 10 mL with deionized water. Then 5 mL of $NaBH_4$ solution was rapidly injected under constant stirring. The yellow color of solution gradually vanished, indicating the reduction of 4-NP. The concentration of 4-NP was determined spectrophotometrically at a wavelength of 400 nm using a Hitachi U-3000 spectrophotometer. For recycling experiment, Au nanocatalyst was colleted by using an external magnetic field after the reaction, washed two times with deionized water, and then reused.

3. Results and discussion

3.1. Basic properties of magnetically recoverable Au nanocatalyst

The abundant nitrogen content of chitosan enables it to effectively uptake high amount of metal ions via ion exchange or chelating processes, depending on the nature of metal ions and the pH of solution [38–40]. Fig. 2 shows the adsorption capacity of chitosan-coated magnetic nanocarrier for Au(III) ions. It was found that the amount of Au(III) ions adsorbed increased with increasing the initial concentration of Au(III) ions. When the initial Au(III) ion concentration was 1000 mg/L, the uptake of Au(III) ions by the chitosan-coated magnetic nanocarrier was more than 95% (4.93 mg). Using the Au(III) ions-adsorbed magnetic nanocarrier obtained under this condition as a source, Au nanoparticles-conjugated magnetic nanocarrier could be effortlessly formed by the addition of reducing agent because the electrostatic attractive force between the amino groups in chitosan and the Au(III) ions in solution provided an effective driving force in the formation and stabilization of these metal nanoparticles [41–44]. Fig. 3 shows the TEM image of the chitosan-coated magnetic nanocarrier after the adsorption–reduction of Au(III) ions. It was obvious that Au nanoparticles with a mean diameter of about 3.14 nm were capped on the surface of chitosan-coated magnetic nanocarrier, revealing that the magnetically recoverable Au nanocatalyst has been successfully fabricated. Since the Au(III) ions adsorbed were reduced

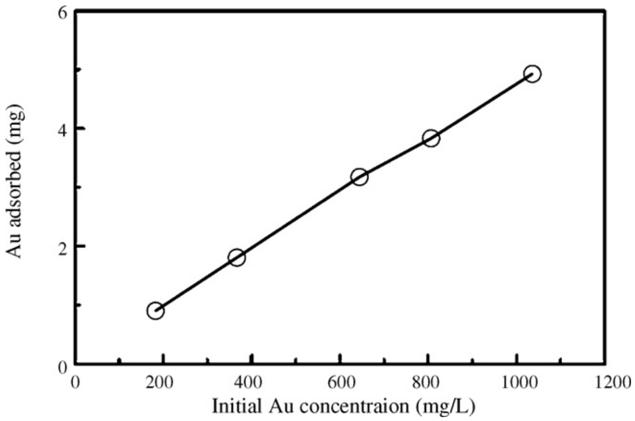

Fig. 2. Effect of initial Au(III) ion concentration on the adsorption amount of Au(III) ions on chitosan-coated magnetic nanocarrier at pH 2 and 25 °C.

to Au nanoparticles completely, the loading of Au nanoparticles on the magnetic carrier could be calculated to be 47 mg/g.

3.2. Catalytic ability of magnetically recoverable Au nanocatalyst for 4-NP reduction

For the study of catalyst-mediated reduction of 4-NP, the reduction process was conducted in the absence of Au nanocatalyst at first. It was observed that the yellow color of solution deepened after the addition of $NaBH_4$ and a red shift of the peak from 317 to 400 nm occurred. This was due to the formation of 4-nitrophenolate ions in alkaline condition by the action of $NaBH_4$ [45]. The intensity of the absorbance remained unchanged at 400 nm even after several days, which revealed that no reduction of 4-NP occurred. However, in the presence of Au nanocatalyst complete reduction of 4-NP to 4-AP by $NaBH_4$ was observed within few minutes (Fig. 4), revealing that the resultant Au nanocatalyst indeed possessed excellent catalytic activity to the reduction of 4-NP. In addition, it was also found that the concentration of 4-NP decreased with time while Au nanocatalyst was replaced by the Au(III) ions-adsorbed magnetic nanocarrier. This was due to the reduction of Au^{3+} to Au^0 by $NaBH_4$ to form Au nanoparticles on the magnetic nanocarrier, leading to the reduction of 4-NP. However, the rate was slower than that obtained in the presence of preformed Au nanocatalyst. This may be attributed to the facts that $NaBH_4$ was partially consumed for the reduction of Au^{3+} to Au^0, less Au nanoparticles were available because they were in situ synthesized during the reaction, and the reduction of 4-NP was initialized after the formation of Au nanoparticles.

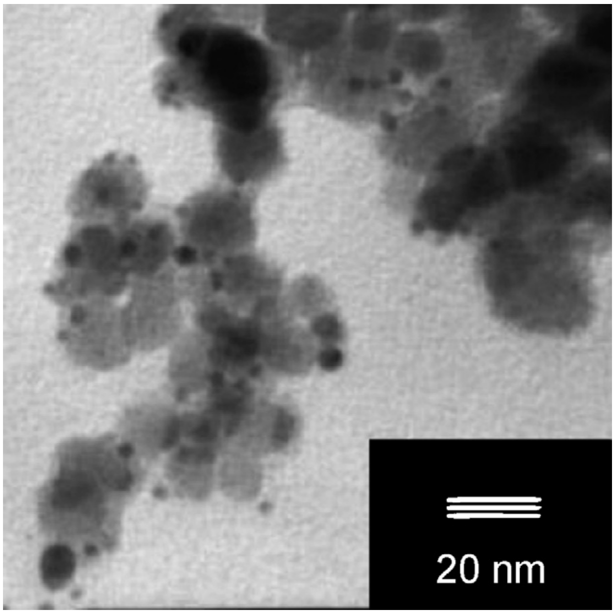

Fig. 3. A typical TEM image of the Au nanoparticles capped on the chitosan-coated magnetic nanocarrier.

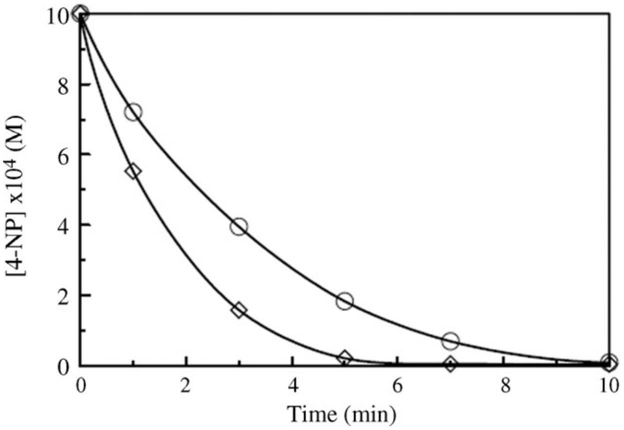

Fig. 4. Plots of 4-NP concentrations at different time intervals during the reduction process with $NaBH_4$ in the presence of Au nanocatalyst (○) or Au(III) ions-adsorbed magnetic nanocarrier (◊). $[Au]_0 = 0.49$ mg, $[4\text{-NP}] = 1 \times 10^{-3}$ M, $[4\text{-NP}]/[NaBH_4] = 0.3$, 30 °C.

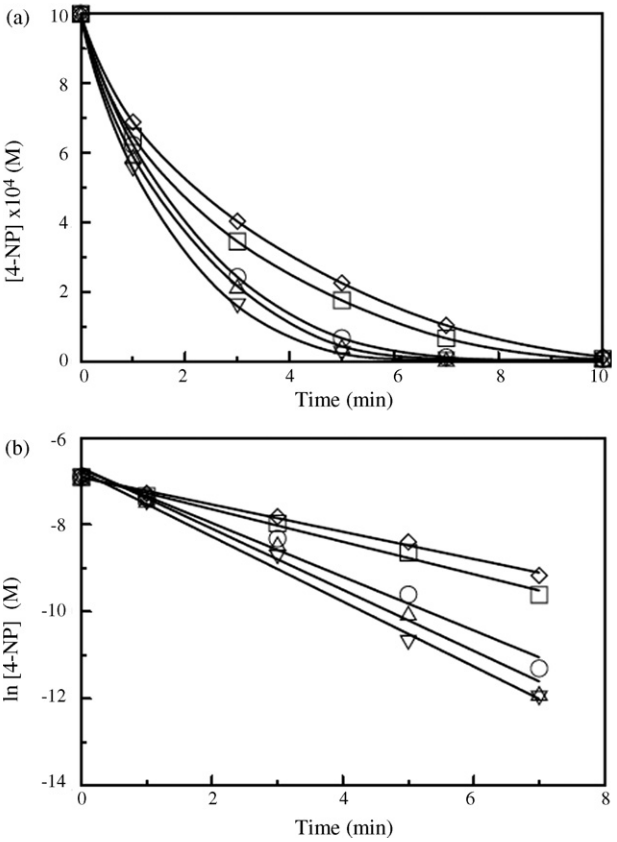

Fig. 5. Plots of the concentration of 4-NP versus time for the reduction of 4-NP with $NaBH_4$ at different amounts of Au nanocatalyst (a) and the plots of ln [4-NP] versus time (b). $[Au]_0 = 0.09$ (◊), 0.18 (□), 0.32 (○), 0.38 (△), and 0.49 (▽) mg. $[4\text{-NP}] = 1 \times 10^{-3}$ M, $[4\text{-NP}]/[NaBH_4] = 0.3$, 30 °C.

Table 1
Pseudo-first-order rate constants and turnover frequencies for the reduction of 4-NP by $NaBH_4$ in the presence of magnetic recoverable Au nanocatalyst.

$10^4 \times$ [4-NP] (M)	$[Au]_0$ (mg)	T (°C)	$10^2 \times k$ (min^{-1})	Correlation coefficient	Turnover frequency (mmol/(g s))
1	0.09	30	31.3	0.995	0.35
1	0.18	30	37.4	0.993	0.18
1	0.32	30	61.8	0.983	0.11
1	0.38	30	70.3	0.983	0.09
1	0.49	30	74.8	0.993	0.07
2	0.49	30	41.7	0.976	0.14
5	0.49	30	38.1	0.980	0.34
10	0.49	30	10.0	0.967	0.38
2	0.49	20	23.0	0.994	0.12
2	0.49	40	88.2	0.957	0.14

3.3. Kinetics for catalytic reduction of 4-NP

Fig. 5(a) shows that the plots of the concentration of 4-NP versus time at different amounts of Au nanocatalyst. It was obvious that the concentration of 4-NP gradually decreased due to the reduction of 4-NP to 4-AP and the reduction rate increased with the increase in the amount of Au nanocatalyst. The plots of ln [4-NP] versus time yielded good linear correlations as indicated in Fig. 5(b), revealing that the $NaBH_4$-reduction of 4-NP catalyzed by Au nanocatalyst followed the pseudo-first-order kinetics. The values of pseudo-first-order rate constants (k), correlation coefficients and turnover frequencies determined were listed in Table 1. These data revealed that pseudo-first-order rate constants increased with increasing the amount of Au nanocatalyst but the turnover frequencies decreased. That is, high catalyst concentration raised the reduction rate of 4-NP but decreased the specific activity of catalyst.

The effects of initial 4-NP concentration and temperature on the reduction of 4-NP with $NaBH_4$ in the presence of Au nanocatalyst were shown in Figs. 6 and 7, respectively. Similar trends as observed in Fig. 5 were obtained. The values of pseudo-first-order rate constants, correlation coefficients and turnover frequencies were also shown in Table 1. It was found that, with the increase in the initial 4-NP concentration, the pseudo-first-order rate constants decreased but the turnover frequencies increased. In addition, the pseudo-first-order rate constants increased with increasing temperature but the turnover frequencies showed no significant changes. By using the Arrhenius equation, the activation energy could be calculated to be 51.2 kJ/mol.

The rate of electron transfer at the metal surface can be influenced by the diffusion of 4-NP to the metal surface, interfacial electron transfer, and the diffusion of 4-AP away from the surface [19]. The observed rate constant can be expressed as [19,46]:

$$\frac{1}{k_{obs}} = \frac{1}{4\pi R^2}\left(\frac{1}{k_{et}} + \frac{R}{D}\right) \tag{1}$$

where R is the radius of metal nanoparticles, D is the diffusion coefficient, and k_{et} is the rate constant for electron transfer. Because smaller metal particles possess higher redox potential value which may accelerate the electron transfer [11], it was assumed that the heterogeneous charge transfer was faster than diffusion for the Au nanoparticles-catalyzed reduction of 4-NP with $NaBH_4$ owing to the small diameter of Au nanoparticles (3.14 nm). Thus, Eq. (1) could be reduced to the Smoluchowski expression:

$$k_{obs} = 4\pi DR \tag{2}$$

The rate constant is proportional to the diffusion coefficient, but the diffusion coefficient is inversely proportional to the concentration of 4-NP and proportional to the square root of temperature [47]. This Smoluchowski expression was consistent with the observations in the studies on the effects of initial 4-NP concentration and temperature. So, it could be recognized that the $NaBH_4$-reduction of 4-NP by the magnetic recoverable Au nanocatalyst developed in this work was diffusion controlled. This was similar to those observed in the reduction of 4-NP by dendrimer encapsulated-metal (Ah, Pt, and Pd) nanoparticles [19], and the diffusion-controlled mechanism could be attributed to the chitosan layer on the surface of iron oxide nanoparticles where Au nanoparticles were formed and stabilized.

3.4. Reusability of magnetically recoverable Au nanocatalyst

Fig. 8 shows the reusability of the magnetically recoverable Au nanocatalyst for the reduction of 4-NP with $NaBH_4$. It was observed

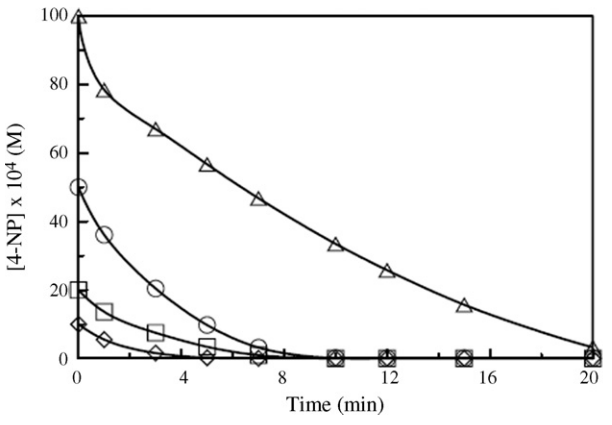

Fig. 6. Plots of the concentration of 4-NP versus time for the reduction of 4-NP with $NaBH_4$ at different initial concentrations of 4-NP. [4-NP] = 1×10^{-3} (◇), 2×10^{-3} (□), 5×10^{-3} (○), 1×10^{-2} (△) M. $[Au]_0$ = 0.49 mg, [4-NP]/[$NaBH_4$] = 0.3, 30 °C.

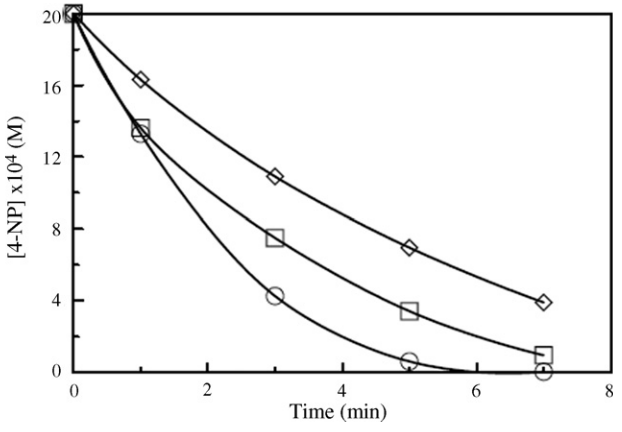

Fig. 7. Plots of the concentration of 4-NP versus time for the reduction of 4-NP with $NaBH_4$ at different temperatures. Temperature = 20 (◇), 30 (□), and 40 (○) °C. $[Au]_0$ = 0.49 mg, [4-NP] = 2×10^{-3} M, [4-NP]/[$NaBH_4$] = 0.3.

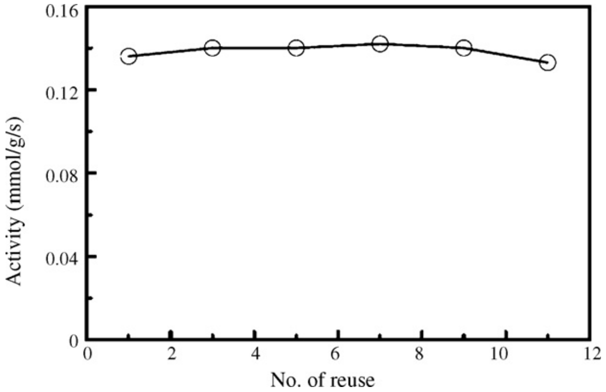

Fig. 8. Reusability of the magnetically recoverable Au nanocatalyst for the reduction of 4-NP with $NaBH_4$. $[Au]_0 = 0.49$ mg, [4-NP] = 2×10^{-3} M, [4-NP]/[$NaBH_4$] = 0.3, 30 °C.

from the recycle study that the efficiency of Au nanocatalyst to reduce 4-NP almost remained unchanged even after the 11th recycle. It could be suggested that the magnetically recoverable Au nanocatalyst was not deactivated or poisoned during the catalytic or separation processes. Also, the Au nanocatalyst could be recovered almost completely. Compared with other metal nanoparticles which are generally oxidized on the surface in alkali condition leading to activity loss [46], the Au nanocatalyst developed in this work was stable and exhibited excellent catalytic ability.

4. Conclusions

A novel magnetically recoverable Au nanocatalyst was fabricated by the adsorption–reduction of Au(III) ions on the chitosan-coated iron oxide nanoparticles. The product could be easily recovered by the application of an external magnetic field and the Au nanoparticles supported on the magnetic nanocarrier had a mean diameter of 3.14 nm. The catalytic ability of the resultant magnetically recoverable Au nanocatalyst was demonstrated by the study on the reduction of 4-NP to 4-AP with $NaBH_4$. The reduction reaction followed the pseudo-first-order kinetics and was diffusion controlled. The rate constant increased while the amount of Au nanocatalyst increased, the initial 4-NP concentration decreased, or the temperature increased. Furthermore, the Au nanocatalyst was found to be quite stable with excellent catalytic ability even after 11 recycles. This work may be useful in developing the process for the conversion of 4-NP to 4-AP in aqueous solution under mild condition, and will be also helpful for the development and applications of magnetically recoverable Au nanocatalysts.

Acknowledgment

This work was performed under the auspices of the National Science Council of the Republic of China, under contract number NSC94-2214-E006-006, to which the authors wish to express their thanks.

References

[1] E. Marais, T. Nyokong, Adsorption of 4-nitrophenol onto Amberlite IRA-900 modified with metallophthalocyanines, J. Hazard. Mater. 152 (2008) 293–301.
[2] O.A. O'Connor, L.Y. Young, Toxicity and anaerobic biodegradability of substituted phenols under methanogenic conditions, Environ. Toxicol. Chem. 8 (1989) 853–862.
[3] M.S. Dieckmann, K.A. Gray, A comparison of the degradation of 4-nitrophenol via direct and sensitized photocatalysis in TiO_2 slurries, Water Res. 30 (1996) 1169–1183.
[4] L.L. Bo, Y.B. Zhang, X. Quan, B. Zhao, Microwave assisted catalytic oxidation of p-nitrophenol in aqueous solution using carbon-supported copper catalyst, J. Hazard. Mater. 153 (2008) 1201–1206.
[5] M.A. Oturan, J. Peiroten, P. Chartrin, A.J. Acher, Complete destruction of *p*-nitrophenol in aqueous medium by electro-Fenton method, Environ. Sci. Technol. 34 (2000) 3474–3479.
[6] N. Modirshahla, M.A. Behnajady, S. Mohammadi-Aghdam, Investigation of the effect of different electrodes and their connections on the removal efficiency of 4-nitrophenol from aqueous solution by electrocoagulation, J. Hazard. Mater. 154 (2008) 778–786.
[7] P. Cañizares, C. Sáez, J. Lobato, M.A. Rodrigo, Electrochemical treatment of 4-nitrophenol-containing aqueous wastes using boron-doped diamond anodes, Ind. Eng. Chem. Res. 43 (2004) 1944–1951.
[8] Y. Du, H. Chen, R. Chen, N. Xu, Synthesis of *p*-aminophenol from *p*-nitrophenol over nano-sized nickel catalysts, Appl. Catal. A: Gen. 277 (2004) 259–264.
[9] M.J. Vaidya, S.M. Kulkarni, R.V. Chaudhari, Synthesis of *p*-aminophenol by catalytic hydrogenation of *p*-nitrophenol, Org. Process Res. Dev. 7 (2003) 202–208.
[10] N. Pradhan, A. Pal, T. Pal, Catalytic reduction of aromatic nitro compounds by coinage metal nanoparticles, Langmuir 17 (2001) 1800–1802.
[11] N.R. Jana, T. Pal, Redox catalytic property of still-growing and final palladium particles: a comparative study, Langmuir 15 (1999) 3458–3463.
[12] S.K. Ghosh, M. Mandal, S. Kundu, S. Nath, T. Pal, Bimetallic Pt–Ni nanoparticles can catalyze reduction of aromatic nitro compounds by sodium borohydride in aqueous solution, Appl. Catal. A 268 (2004) 61–66.
[13] N.R. Jana, T.K. Sau, T. Pal, Growing small silver particle as redox catalyst, J. Phys. Chem. B 103 (1999) 115–121.
[14] T.K. Sau, A. Pal, T. Pal, Size regime dependent catalysis by gold nanoparticles for the reduction of eosin, J. Phys. Chem. B 105 (2001) 9266–9272.
[15] N.R. Jana, Z.L. Wang, T. Pal, Redox catalytic properties of palladium nanoparticles: surfactant and electron donor–acceptor effects, Langmuir 16 (2000) 2457–2463.
[16] S.K. Ghosh, S. Kundu, M. Mandal, T. Pal, Silver and gold nanocluster catalyzed reduction of methylene blue by arsine in a micellar medium, Langmuir 18 (2002) 8756–8760.
[17] K. Esumi, K. Miyamoto, T. Yoshimura, Comparison of PAMAM–Au and PPI–Au nanocomposites and their catalytic activity for reduction of 4-nitrophenol, J. Colloid Interface Sci. 254 (2002) 402–405.
[18] K. Hayakawa, T. Yoshimura, K. Esumi, Preparation of gold–dendrimer nanocomposites by laser irradiation and their catalytic reduction of 4-nitrophenol, Langmuir 19 (2003) 5517–5521.
[19] K. Esumi, R. Isono, T. Yoshimura, Preparation of PAMAM- and PPI-metal (silver, platinum, and palladium) nanocomposites and their catalytic activities for reduction of 4-nitrophenol, Langmuir 20 (2004) 237–243.
[20] Y.C. Chang, D.H. Chen, Preparation and adsorption properties of monodisperse chitosan-bound Fe_3O_4 magnetic nanoparticles for removal of Cu (II) ions, J. Colloid Interface Sci. 283 (2005) 446–451.
[21] Y.C. Chang, S.W. Chang, D.H. Chen, Iron oxide-supported chitosan nanoparticles: studies on chitosan binding and adsorption of Co (II) ions, React. Funct. Polym. 66 (2006) 335–341.
[22] Y.C. Chang, D.H. Chen, Recovery of gold (III) ions by a chitosan-coated magnetic nano-adsorbent, Gold Bull. 39 (3) (2006) 98–102.
[23] Y.C. Chang, D.H. Chen, Adsorption kinetics and thermodynamics of acid dyes on a carboxymethylated chitosan-conjugated magnetic nano-adsorbent, Macromol. Biosci. 5 (2005) 254–261.
[24] Y.C. Chang, D.B. Shieh, C.H. Chang, D.H. Chen, Conjugation of monodisperse chitosan-bound magnetic nano-carrier with epirubicin for targeted cancer therapy, J. Biomed. Nanotechnol. 1 (2005) 196–201.
[25] A. Kondo, H. Fukuda, Preparation of thermo-sensitive magnetic hydrogel microspheres and application to enzyme immobilization, J. Ferment. Bioeng. 84 (1997) 337–341.
[26] S.M. O'Brien, R.P. Sloane, O.R.T. Thomas, P. Dunnill, Characterisation of non-porous magnetic chelator supports and their use to recover polyhistidine-tailed T4 lysozyme from a crude *E. coli* extract, J. Biotechnol. 54 (1997) 53–67.
[27] P.R. Levison, S.E. Badger, J. Dennis, P. Hathi, M.J. Davies, I.J. Bruce, D. Schimkat, Recent developments of magnetic beads for use in nucleic acid purification, J. Chromatogr. A 816 (1998) 107–111.
[28] R. Abu-Reziq, H. Alper, D. Wang, M.L. Post, Metal supported on dendronized magnetic nanoparticles: highly selective hydroformylation catalysts, J. Am. Chem. Soc. 128 (2006) 5279–5282.
[29] R. Zanella, S. Giorgio, C.R. Henry, C. Louis, Alternative methods for the preparation of gold nanoparticles supported on TiO_2, J. Phys. Chem. B 106 (2002) 7634–7642.
[30] A. Wolf, F. Schuth, A systematic study of the synthesis conditions for the preparation of highly active gold catalysts, Appl. Catal. A: Gen. 226 (2002) 1–13.
[31] M. Haruta, Gold as a low-temperature oxidation catalyst: factors controlling activity and selectivity, Stud. Surf. Sci. Catal. 110 (1997) 123–134.
[32] M. Haruta, Gold as a novel catalyst in the 21st century: preparation, working mechanism and applications, Gold Bull. 37 (2004) 27–36.
[33] R. Meyer, C. Lemire, S.K. Shaikhutdinov, H.J. Freund, Surface chemistry of catalysis by gold, Gold Bull. 37 (2004) 72–124.
[34] P.L. Freund, M. Spiro, Colloidal catalysis: the effect of sol size and concentration, J. Phys. Chem. 89 (1985) 1074–1077.
[35] D.S. Miller, A.J. Bard, G. Mclendon, J. Ferguson, Catalytic water reduction at colloidal metal "microelectrodes". 2. Theory and experiment, J. Am. Chem. Soc. 103 (1981) 5336–5341.

[36] Z.J. Jiang, C.Y. Liu, L.W. Sun, Catalytic properties of silver nanoparticles supported on silica spheres, J. Phys. Chem. B 109 (2005) 1730–1735.
[37] S. Preharaj, S. Nath, S.K. Ghosh, S. Kundu, T. Pal, Immobilization and recovery of Au nanoparticles from anion exchange resin: resin-bound nanoparticle matrix as a catalyst for the reduction of 4-nitrophenol, Langmuir 20 (2004) 9889–9892.
[38] R.S. Juang, H.J. Shao, A simplified equilibrium model for sorption of heavy metal ions from aqueous solutions on chitosan, Water Res. 36 (2002) 2999–3008.
[39] J.C.Y. Ng, W.H. Cheung, G. McKay, Equilibrium studies of the sorption of Cu (II) ions onto chitosan, J. Colloid Interface Sci. 255 (2002) 64–74.
[40] K. Inoue, K. Yoshizuka, K. Ohto, Adsorptive separation of some metal ions by complexing agent types of chemically modified chitosan, Anal. Chem. Acta 388 (1999) 209–218.
[41] H. Huang, Y. Qiang, X. Yang, Morphology study of gold–chitosan nanocomposites, J. Colloid Interface Sci. 282 (2005) 26–31.
[42] H. Huang, Y. Qiang, X. Yang, Preparation and characterization of metal–chitosan nanocomposites, Colloids Surf. B Biointerfaces 39 (2004) 31–37.
[43] H. Huang, X. Yang, Synthesis of chitosan-stabilized gold nanoparticles in the absence/presence of tripolyphosphate, Biomacromolecules 5 (2004) 2340–2346.
[44] Z. Li, Y. Du, Biomimic synthesis of CdS nanoparticles with enhanced luminescence, Mater. Lett. 57 (2003) 2480–2484.
[45] N. Pradhan, A. Pal, T. Pal, Silver nanoparticle catalyzed reduction of aromatic nitro compounds, Colloids Surf. A Physicochem. Eng. Aspects 196 (2002) 247–257.
[46] M. Grátzel, A.J. Frank, Interfacial electron-transfer reactions in colloidal semiconductor dispersions. Kinetic analysis, J. Phys. Chem. 86 (1982) 2964–2967.
[47] K.J. Laidler, J.H. Meiser, B.C. Sanctuary, Physical Chemistry, fourth ed., Houghton Mifflin Company, Boston, 2003, p. 983.